Kohn-Luttinger Interference Effect and Location of the Conduction-Band Minima in 6H SiC

Lyle Patrick

Westinghouse Research Laboratories, Pittsburgh, Pennsylvania 15235

Recent Raman-scattering results place the conduction-band minima of 6H SiC on the M-L symmetry line, leaving undetermined the parameter k_z that is required to fix their positions exactly. This parameter could be established by electron-nuclear-double-resonance (ENDOR) measurements, as a similar parameter is for Si, but the present ENDOR results for 6H SiC are insufficient. The Raman result determines the planar part of the donor Kohn-Luttinger interference pattern, and it is found that the highly symmetric pattern concentrates the donor-electron density on lattice sites of planes *like* the donor plane. Because of the Bloch portion of the wave function, this leads to binding-energy differences for the three inequivalent nitrogen donors, for each donor has a distinct set of neighboring *like* planes. Whether or not a *like* plane is favorably placed for a binding-energy enhancement depends on the axial interference factor, which is a function of k_z. Thus, an interpretation of the donor binding energies is used to determine k_z. The suggested k_z is one for which 6H SiC has six conduction-band minima.

I. INTRODUCTION

Valley-orbit Raman transitions, $1s(A_1) \rightarrow 1s(E_2)$, have recently been observed by Colwell and Klein[1] for N donors in 6H SiC, which is a many-valley semiconductor with the same space group as wurtzite, $P6_3mc$. The Raman results require that the conduction-band minima lie on the M-L symmetry lines, leaving undetermined the axial components of their positions $\pm k_z$. There is evidence that the minima do *not* lie at M, which is a critical point by symmetry.[2] These conclusions are in good agreement with a proposal by Herman *et al.*[3] Their band calculation for 2H SiC showed a set of secondary minima along M-L, and they suggested that these become primary minima in 6H and some other SiC polytypes.

The situation is similar to that in Si, where the minima lie along the Δ axis, and a parameter $k_0/k_{\max}$ is needed to fully define the positions. In Si, Feher[4] and others[5,6] have used electron-nuclear double resonance (ENDOR) to sample the complex donor-electron density pattern that results from the Kohn-Luttinger interference effect.[7] The results are interpreted to determine the positions of the minima within close limits. The same procedure could be applied to 6H SiC to determine k_z, but the reported ENDOR results are insufficient for this purpose.[8] The best present means of investigating the electron-density variation in 6H SiC is an interpretation of the electron binding energies at the three inequivalent nitrogen donors.[9]

The fact that N-donor ionization energies vary from 0.17 to 0.23 eV is at first sight rather surprising, for the tetrahedral bond lengths at the three sites differ by only one part per thousand,[10]

and the hyperfine splittings in the electron paramagnetic resonance[11] vary by only 1%. Thus, the sites appear to be nearly identical, and the differences in energies cannot be attributed to differences in central-cell corrections.[7] It is significant that the orbital radius of the N-donor electron is about 5 Å, whereas the unit-cell axial dimension is 15.1 Å.[12] Thus, electrons bound at different sites sample somewhat different portions of the lattice. Since the electron effective mass is determined by the electron-lattice interaction, one could say that there is a different effective mass for each of the three N donors. However, it is more useful to examine the lattice differences in donor neighborhoods for configurations that augment the binding energy by increasing the effectiveness of the Bloch portion of the wave function.

A result of the hexagonal symmetry is that the Kohn-Luttinger interference factor can be written as a product of axial and planar factors. The knowledge that the conduction-band minima lie on the M-L axis is sufficient to determine the planar interference factor, and it shows that the electron density is enhanced at lattice sites in planes *like* that in which the donor lies. The degree of enhancement depends on the known disposition of *like* planes about a donor, and on the unknown axial interference factor, which is a function of k_z. Thus, it is possible to plot the enhancement effect against k_z for each donor. A comparison with the known binding energies then enables us to suggest a location for the conduction-band minima.

We discuss the Raman results in Sec. II and the application of the calculated 2H band structure to polytype 6H in Sec. III. The A_1 and E_2 interference patterns due to the planar portion of the Kohn-Luttinger effect are then shown in Sec. IV, and

their enhancement at lattice sites on planes *like*
the donor plane is considered. The two-dimension-
al sublattice of the interference maxima in $6H$ is
compared with the three-dimensional interference
sublattice of cubic SiC. The $6H$ lattice structure
about each of the three donor sites is discussed in
Sec. V, and experimental information is used in
Sec. VI to suggest a value of k_z.

II. RAMAN-SCATTERING RESULTS

Colwell and Klein studied the low-temperature
Raman scattering of nitrogen-doped $6H$ SiC.[1] They
found three lines of E_2 symmetry which they at-
tributed to excitation within the valley-orbit split
$1s$ group, one line for each of the three inequiva-
lent N donors. The ground states must be A_1, for
all three N donors show hyperfine splitting in EPR.[11]
Thus the Raman transitions are $1s(A_1) \rightarrow 1s(E_2)$. No
excitation with E_1 symmetry was found. The N do-
nors are at sites of C_{3v} symmetry, but the observa-
tion of E_2 transitions and not E_1 indicates that the
macroscopic symmetry of the crystal, C_{6v}, is more
appropriate for this problem.

Figure 1 shows the Brillouin zone for the wurtzite
structure. The Brillouin zone for $6H$ SiC is identi-
cal, except that the axial dimension is reduced by a
factor of 3. The positions of the conduction-band
minima in the zone determine what $1s$ representa-
tions are available for Raman excitation. All pos-
sible positions will be examined, but we need con-
sider only node-free conduction-band states, for
only they can form an A_1-donor ground state.

The crystal symmetry induces a star of minima
for each position considered. Under the opera-
tions of C_{6v} the characters of a reducible represen-
tation are determined for each star, and the ir-
reducible representations of a $1s$ state can then be
found by inspection. The results are shown in Ta-
ble I for all positions within the plane $k_z = 0$.

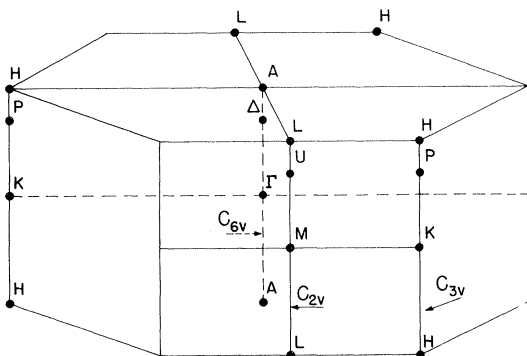All symmetry operations of C_{6v} leave k_z un-

FIG. 1. Brillouin zone for the wurtzite lattice, with
the standard notation for points and lines of symmetry.
Three kinds of symmetry lines parallel to the axis are
indicated by the corresponding point-group symbols.

changed; hence the results for the plane $k_z = 0$ are
sufficient to determine the irreducible representa-
tions of the donor $1s$ states for any position in the
Brillouin zone. For minima with $k_z \neq 0$ or $\pm \pi/c$
there are two planes of minima with $\pm k_z = $ const.
There is then a doubling of (a) the number of mini-
ma, (b) the characters in the reducible representa-
tion of the star, and (c) the number of each type of
irreducible representation. However, it will be
shown later that these doublings do *not* introduce
any additional possibilities for Raman scattering;
hence the observation of a single transition does not
exclude a general value of k_z.

For comparison with the experimental results, we
look for the presence of E_2 and the absence of E_1.
Table I indicates that only the position M satisfies
this requirement. Since k_z is not determined, we
place the $6H$ conduction-band minima on the line
M-L, as suggested by Colwell and Klein. There are
three minima if they are at M or L, but six for a
general position U on the line M-L. One objective
of this paper is to use other experimental infor-
mation to make an approximate determination of k_z.

III. POLYTYPE COMPARISONS

The conduction-band minima in $3C$ SiC (zinc
blende) are known to be at X. Phonon-assisted
transitions in the luminescence of bound excitons
therefore enable us to measure the $3C$ phonon en-
ergies at X.[13] In $6H$ SiC exciton luminescence,[14]
the principal phonon energies are found to be simi-
lar to those of $3C$, suggesting that the conduction-
band minima of $6H$ are in positions that are com-
parable with the X positions of $3C$.

Comparable positions in the zinc-blende and
wurtzite zones have been discussed by several au-
thors.[3,15] To compare $3C$ and $6H$ SiC in the same
way, zones of equal volume must be used, and that
is most easily accomplished by extending the $6H$ SiC
zone to $6\pi/c$ in the axial direction. In the present
case we need compare only mirror planes, por-
tions of which are shown in Fig. 2, for X in $3C$ and
the line M-L in $6H$ both lie in these equivalent
planes. Figure 2 shows that the cubic X position
falls at one of the M positions of $6H$ $[M(4\pi/c)]$.
There are planes of energy discontinuity within the
large zone of $6H$, and traces of these planes are
indicated by the solid Γ-M lines. However, these
discontinuities are expected to be very small, for
they are due to minor differences in the nearly
equivalent planes that are stacked perpendicular to
the c axis. The corresponding discontinuities in
the phonon-dispersion curves are less than 1 meV.[16]
The dotted lines A-L do not represent discontinui-
ties, for the crystal symmetry requires degener-
acies at L.[2,17]

We now turn to energy-band calculations for $2H$
SiC by Herman *et al.*[3] They show the lowest minima

TABLE I. The irreducible representations of donor $1s$ states for all possible symmetry positions of the conduction-band minima in the $k_z = 0$ plane of the $6H$ SiC Brillouin-zone.

Position of minima	Number of minima	$1s$ states
Γ	1	A_1
K	2	$A_1 B_2$
M	3	$A_1 E_2$
$\Gamma - K$	6	$A_1 B_2 E_1 E_2$
$\Gamma - M$	6	$A_1 B_1 E_1 E_2$
$M - K$	6	$A_1 B_2 E_1 E_2$
General	12	All

at K, in agreement with the exciton-luminescence results for $2H$.[18] Secondary minima appear on the line M-L. Their lowest M-L conduction bands have been unfolded in Fig. 3(a) to span the axial dimension M-L-M appropriate for the large zone, with M_1 at $k_z = 0$, as required for an A_1-donor ground state. The position corresponding to X in $3C$ is indicated.

The $2H$ band has been modified to make a schematic $6H$ band in Fig. 3(b) by introducing small energy gaps at the M positions that fall within the large zone. The minimum has also been displaced to what we shall later suggest is the approximate position in $6H$, based on the Kohn-Luttinger interference effect. In making these modifications we are motivated by the suggestion of Herman *et al.* that the $2H$ secondary minima become the primary minima of $6H$ and some other polytypes. The Raman-scattering results of Colwell and Klein provide strong support for this proposal.

IV. KOHN-LUTTINGER INTERFERENCE EFFECT

For a many-valley semiconductor, the Kohn-Luttinger donor wave function[7] is written as a sum over all minima,

$$\psi = \sum_j \alpha^j F^j(\vec{r}) u_k^j(\vec{r}) e^{i \vec{k}^j \cdot \vec{r}} . \tag{1}$$

For the jth portion, α^j is a numerical coefficient, F^j is an envelope function, and the remainder is a Bloch function. The $1s(A_1)$ ground state is formed by taking equal α^j. We neglect the dependence of F and u on j in order to study the strong electron-density variation due to S^2, the square of the interference factor

$$S = \sum_j \alpha^j e^{i \vec{k}^j \cdot \vec{r}} . \tag{2}$$

For $6H$ SiC, the vector $\vec{k}^j$ can be written as a sum of axial and planar parts, k_z^j and $\vec{k}_p^j$, and the Raman-scattering results show that $\vec{k}_z^j = \vec{k}_M^j$. This decomposition permits us to write S as a product of axial and planar interference factors, $S = S_z S_p$, and the pairing of $\pm k_z$ terms yields

$$S_z = \sqrt{2} \cos k_z z . \tag{3}$$

In addition, each $\pm \vec{k}_M$ can be paired to form a standing wave, although $\pm \vec{k}_M$ differ by a reciprocal-lattice vector and therefore represent a single minimum. The result for the planar interference factor of the A_1 state is

$$S_p(A_1) = (1/\sqrt{3}) \sum_j \sqrt{2} \cos \vec{k}_M^j \cdot \vec{p} , \quad j = 1, 2, 3 \tag{4}$$

in which $\vec{k}_M$ and $\vec{p}$ are two-dimensional vectors in the plane, and the sum is over the three minima in the star of M.

A. Planar Interference Pattern for A_1

The axial-stacking order of double planes (Si and C) in $6H$ SiC can be written $ABCACB$.[19] Because S_p is independent of z, the phase relations at lattice sites must be the same in all planes that differ only by an axial displacement. Then, if the donor is in an A plane, all other A planes are *like* (L) planes. The B and C planes are *unlike* (U) planes, being equivalent to each other with respect to S_p because of the hexagonal symmetry. Thus, the relationship of S_p to lattice sites takes only two forms, L and U, and these can both be seen in Fig. 4, which shows the interference pattern generated by $S_p(A_1)$.

The projections of lattice sites on the plane of the donor are shown in Fig. 4 as filled circles for L planes and as open circles for U planes. Only one of the two equivalent sets of U positions is shown. Each solid line is a line of $(360n)°$ phase for one of the three terms of Eq. (4), where n is an integer (including zero). Each dashed line is a line of $(180m)°$ phase, where m is an odd integer. S_p is evaluated at each lattice site and different circle sizes are used in Fig. 4 to distinguish different values. The four values of S_p^2 are listed at the
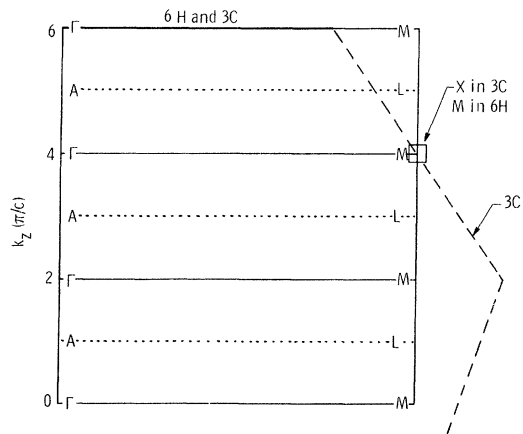

FIG. 2. Parts of the large-zone mirror planes for $3C$ and $6H$ SiC. The planes coincide over much of the drawing, but differ at the right, where the dashed line is the $3C$ boundary. The position X in $3C$ is shown by the square, and it corresponds to an M position $6H$.
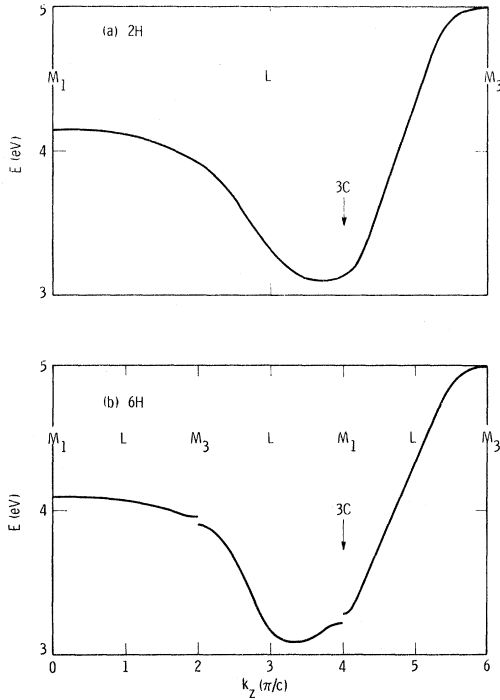
FIG. 3. Energy bands along M-L in $2H$ SiC. (a) The $2H$ band of Ref. 3, unfolded to span the large zone. (b) Schematic $6H$ band, made by introducing appropriate gaps into the $2H$ band, and by displacing the minimum slightly.

right. The donor is at one of the large filled circles, for each cosine term in Eq. (4) is equal to unity at the origin.

Average values of S_p^2 over all atoms in the plane are 2 for L planes and $\frac{1}{2}$ for U planes. The high concentration of electron density on L lattice sites, and the low concentration on U sites, has important consequences for the binding energies of electrons at the three inequivalent N-donor sites.

B. Interference Sublattices

The high symmetry of band minima at M results in a two-dimensional sublattice of maximum electron density at $\frac{1}{4}$ of the lattice sites on L planes, as shown by the large filled circles in Fig. 4. If k_z were $4\pi/c$, corresponding to the X minima of $3C$, then the wavelength in the axial direction would be $c/2$, which is three times the interplanar distance $c_1 = 2.52$ Å. For the ABC axial stacking of planes in $3C$ this combines with the planar sublattice to form a three-dimensional sublattice of interference maxima. In $3C$ the X_1 symmetry of the band minima first confines the s-like portion of the wave function to the fcc C sublattice. If the donor substitutes for C, its Kohn-Luttinger interference factor then results in electron-density maxima on one of the four sc components of the C sublattice.[20] This electron-density structure may have observable

consequences for a donor-acceptor pair spectrum of type I, for the acceptor then occupies a site at an interference maximum of the donor if the shell number m is even. The resulting strong electron-hole overlap should reduce the recombination time, and at high excitation intensity the even-m lines should be relatively stronger than the odd-m lines. The enhanced even/odd ratio would not be observed at low excitation, for the line strength is then determined by the capture time.[21,22]

C. Planar Interference Pattern for E_2

For the $1s(E_2)$ state there is a different interference factor, which we can take as

$$S_p(E_2) = \cos\vec{k}_1\cdot\vec{p} - \cos\vec{k}_2\cdot\vec{p} , \qquad (5)$$

where $\vec{k}_1$ and $\vec{k}_2$ are the wave vectors of any two of the three M positions. The interference pattern again has its origin at the donor site, but its value is zero there because of the cancellation of the two terms in Eq. (5). The phase relations of $S_p(E_2)$ at sites in L and U planes are shown in Fig. 5, where the solid and dashed lines of constant phase have the same meaning as in Fig. 4. S_p^2 values are again shown at the right. Different choices of $\vec{k}_1$ and $\vec{k}_2$ give interference patterns that differ by rotations of $\pm 120°$. This can change the value of S_p^2 at a particular atom, but the sum of S_p^2 remains unchanged over each shell of atoms. In this context, a shell means a set of atoms in the plane that are equidistant from the donor.

The average values of $S_p^2(E_2)$ over all atoms in the plane is 2 for L planes and $\frac{1}{2}$ for U planes, the same as for $S_p^2(A_1)$. Thus, L planes are favored
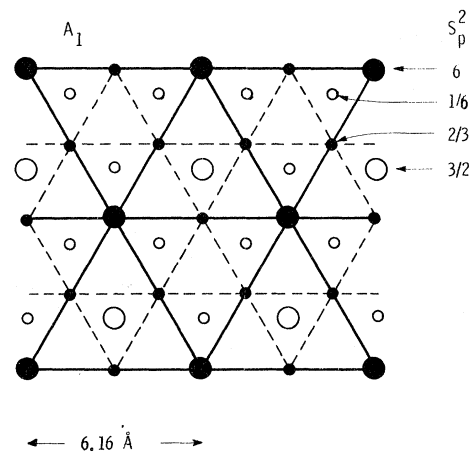

FIG. 4. A_1 interference pattern [Eq. (4)]. Solid lines are lines of $(360n)°$ phase, with n an integer. Dashed lines are lines of $(180m)°$ phase, with m an odd integer. Solid (open) circles are projections of lattice sites in L (U) planes. Two different values of S_p^2, in both L and U planes, are shown by different circle sizes, and the values are shown at the right.

FIG. 5. E_2 interference pattern [Eq. (5)]. Lines and circles have the same meanings as in Fig. 4. Values of S_p^2 are shown at the right.

by both A_1 and E_2 interference patterns, and the origin of *differences* in A_1-E_2 splittings is not evident. The donor central-cell correction of the A_1 wave function can only account for the part of the A_1-E_2 interval that is independent of the donor site. However, it will be shown later that the envelope-function restriction of the wave function to atoms near the donor leads to A_1-E_2 differences on L planes. An L atom with only axial displacement from the donor is especially significant for these differences.

D. Other A_1 and E_2 States

In pairing $\pm k_z$ and $\pm \vec{k}_M$ we used the cosine terms because they give a nonvanishing electron density at the nucleus, as required by the observation of hyperfine splitting in EPR. It is of interest to consider the sine terms also. In the case of the $\pm \vec{k}_M$ pair, the sine term refers to a higher conduction band that has M_3 symmetry at $k_z = 0$.[23] In the case of the $\pm k_z$ pair, however, the sine term also has A_1 symmetry, and the S_z formed from it can be multiplied by S_p terms of A_1 or E_2 symmetry to give another set of $1s(A_1)$ and $1s(E_2)$ valley-orbit states, as required for a six-valley semiconductor. However, in summing over j, the rule cited by Wright and Mooradian[24] shows that Raman transitions to these states have vanishing intensity. Thus, the observation of only a single E_2 Raman line for each donor is to be expected, and does not serve to distinguish between the possibilities of three valleys (at M or L) or six valleys (at a general position on the line M-L).

E. Origin of Enhanced Binding

We now consider how binding energies are affected by the presence of L or U planes in the neighborhood of the donor. The s-like part of the donor wave function is concentrated at lattice sites r_i by the function $u_k(r)$, which has the lattice translation-

al symmetry and has large values at lattice sites. The enhancement factor $u_k^2(r_i) \equiv \eta$ is about 180 for Si.[5] The values $\eta(Si)$ and $\eta(C)$ at Si and C sites in $6H$ SiC are unknown,[25] but we can assume that there is a sizable enhancement, and that it increases the electron binding energy. As we showed, the electron density is concentrated at lattice sites in L planes by S_p, permitting the factors η to operate more effectively.

In Sec. V it will be shown that each of the three N donors has a distinct set of neighboring L planes associated with it. Si and C planes will be considered separately to avoid any assumption about the relative values of $\eta(Si)$ and $\eta(C)$. After weighting the planes for their distances from the donor, the enhancement factors for Si and C planes, for each donor, can be plotted as a function of k_z. The known exciton binding energies are then compared with the enhancement-factor plots to find a satisfactory value of k_z for $6H$ SiC.

V. NITROGEN DONORS

The SiC polytypes differ only in the stacking order of planes along the c axis ($\langle 111 \rangle$ in $3C$). The $ABCACB$ stacking of $6H$ is easily visualized by looking at the atoms in a $(11\bar{2}0)$ mirror plane, as shown in Fig. 6, where the total height is the lattice constant $c = 15.1$ Å. The three inequivalent carbon sites, at which nitrogen may be substituted, are numbered. The two sets of three are equivalent under the 6_3 operation. In this picture atoms vertically above or below a donor site are representatives of L planes, and the various distances to L planes can be noted by repeating the unit cell where necessary. To avoid fractions these distances, listed in Table II, are measured in units of $c/24$, or $c_1/4$, where $c_1 = 2.52$ Å is the axial distance between Si planes (or C planes). Planes beyond 10.08 Å are not listed. The scale at the left of Fig. 6

FIG. 6. Portion of $(11\bar{2}0)$ mirror plane of $6H$ SiC, showing the $ABCACB$ stacking. The lattice constants are $a = 3.08$ Å, $c = 15.1$ Å. One unit-cell height is shown, divided into 24 parts on the scale at the left. The donor N substitutes on the three inequivalent numbered C sites. Distances from each donor to nearby L planes are measured vertically, and are listed in Table II.

also shows the position of each plane, with short scale marks for C, and long for Si.

The Si L planes at $3c_1/4$ do not contribute to donor differences, for they are common to all three. However, all the other L planes must be considered, each weighted for its distance from the donor and for S_z^2, the square of the axial interference factor. The latter being unknown, we obtain the sum over L planes as a function of the parameter k_z. The experimental data on the three N donors are shown in Table III. The problem is to use the L-plane-enhancement effect to assign each energy to a particular site, and to select a value of k_z that fits the data.

Until now we have considered each L plane as a whole. However, the number of atoms that interact significantly with the donor electron is limited by the small orbital radius. Using a dielectric constant of 9.8,[26] and the free-electron mass for the unknown effective mass, we obtain a Bohr radius of 5.2 Å. This radius can be substituted in the envelope function (assumed to be isotropic) to calculate a factor ρ that is proportional to the electron density,

$$\rho = S_p^2 e^{-2r/5.2} . \tag{6}$$

The calculation is made for several shells of atoms in the C plane at $8c_1/4$, an important L plane for the donors N_2 and N_3. The values of ρ are shown in Table IV for both A_1 and E_2 states. The unique atom L_1 has only an axial displacement from the donor ($8c_1/4 = 5.04$ Å). The other shells are numbered in order of their distance, and a total of 19 atoms is considered. For the N_1 donor the plane at 5.04 Å is a U plane, and the comparable values of ρ are shown for the nearest 18 atoms.

There are significant differences between electron-density factors for a limited portion of a plane and their averages over the whole plane. The condition $\rho(L) \gg \rho(U)$ is not changed much (the average L/U ratio for the whole plane is 4 for both A_1 and E_2), but the nearest atom L_1 is very effective in making $\rho[L(A_1)] > \rho[L(E_2)]$, whereas the S_p^2 averages over the plane are equal for A_1 and E_2.

The $1s(A_1)$-$1s(E_2)$ differences shown in Table III are made up of two parts, the central-cell correction and the Kohn-Luttinger enhancement. The

TABLE II. Distances from each of the three N-donor sites to neighboring planes *like* the donor plane, in units of $c/24$. N substitutes for C, and the numbering of the N donors is the same as that of C sites in Fig. 6.

Site	Carbon L planes	Silicon L planes
N_1	12, 12	3, 9, 15
N_2	8, 16	3, 11, 13
N_3	8, 16	3, 5

TABLE III. Experimental data on binding energies at the three N donors. The ionization energies are partly estimated.

Measurement	Energies (meV)
Exciton binding energies	16, 31, 32.5[a]
A_1-E_2 intervals	13.0, 60.3, 62.6[b]
Ionization energies	170, 200, 230[c]

[a]Reference 14.   [b]Reference 1.   [c]Reference 9.

former is approximately the same for all donors, as indicated by the hyperfine splitting; hence the latter must be quite different. Because no differences are seen when averages over planes are considered, the A_1-E_2 intervals must be quite sensitive to the size of the orbit, about which our knowledge is very limited. We shall therefore not use the A_1-E_2 data in evaluating k_z for the conduction-band minima.

We also shall not use the donor ionization energies. They are based on experimental measurements, but portions had to be estimated.[27] Also, like A_1-E_2 differences, they refer to an electron rather strongly bound to a donor. On the other hand, the exciton binding energies are accurately known, and the weak binding means that the electrons are more likely to respond like conduction-band electrons. We need only assume that each bound-electron wave function is a sum over the conduction-band minima in order to form a Kohn-Luttinger interference pattern. It does not even matter whether the function has A_1 or E_2 symmetry, for both enhance the density at lattice sites on L planes, and that is all the information that we shall use.

VI. LOCATION OF CONDUCTION-BAND MINIMA

We now examine the effect of the axial interference factor S_z. The carbon L planes are considered first, and the value of S_z^2 is calculated as a function of k_z for $z = 8$, 12, and 16 in the units of Table II. The results are shown in Fig. 7 for the interval $3\pi/c$ to $5\pi/c$, which spans the neighborhood corresponding to the $3C$ minimum at $4\pi/c$. The enhancement effect of a particular L plane is seen to be strongly dependent on k_z.

The bound-exciton orbital size is not known, but the exciton binding energies do not involve A_1-E_2 differences, so it is not necessary to use an envelope function to weight each shell of atoms separately. Instead, an approximate weighting factor is used for each plane, i.e., a reduction by a factor of 2 for each additional distance of 2.52 Å from the donor. The relative weights for the planes at $c_1/4$ distances of 8, 12, and 16 are therefore 1, 0.5, and 0.25.

A sum over the appropriately weighted C planes (Table II) is made for each N donor, and the re-

TABLE IV. Values of the electronic-density factor ρ for several planar shells of atoms at distances r from the donor, the distance in the plane being p and the axial distance a constant $z = 5.04$ Å. The factor e^{-x} (with $x = 2r/5.2$) is the envelope-function adjustment. Values of S_p^2 are from Figs. 4 and 5, and for E_2 they are averaged over the shell. Total ρ's are for 19 L atoms or 18 U atoms.

Atoms	p (Å)	r (Å)	e^{-x}	$S_p^2(A_1)$	$\rho(A_1)$	$S_p^2(E_2)$	$\rho(E_2)$
$1L_1$	0	5.04	0.144	6	0.86	0	0
$6L_2$	3.08	5.91	0.103	$\frac{2}{3}$	0.41	$\frac{8}{3}$	1.65
$6L_3$	5.33	7.33	0.060	$\frac{2}{3}$	0.24	$\frac{8}{3}$	0.96
$6L_4$	6.16	7.96	0.047	6	1.69	0	0
L totals					3.20 [$L(A_1)$]		2.61 [$L(E_2)$]
$3U_1$	1.78	5.35	0.127	$\frac{1}{6}$	0.06	$\frac{2}{3}$	0.25
$3U_2$	3.56	6.17	0.093	$\frac{3}{2}$	0.42	0	0
$6U_3$	4.70	6.89	0.070	$\frac{1}{6}$	0.07	$\frac{2}{3}$	0.28
$6U_4$	6.41	8.15	0.044	$\frac{1}{6}$	0.04	$\frac{2}{3}$	0.18
U totals					0.59 [$U(A_1)$]		0.71 [$U(E_2)$]

sults are shown in Fig. 8(a). The N_1 curve, for example, is obtained by taking the $z = 12$ curve of Fig. 7 twice as indicated by Table II, and then using the weight factor 0.5. Thus, N_1 is the same as $z = 12$ in Fig. 7. The N_2 and N_3 curves are identical because their carbon L planes are the same. These curves indicate the approximate relative exciton-binding enhancement vs k_z for each of the three inequivalent donors, calculated for the carbon L planes only.

The same procedure is then used to calculate the weighted sum over Si planes for each donor, and the result is shown in Fig. 8(b). The N_3 curve is dominant over much of the range of k_z because of the nearby silicon L plane at $5c_1/4$. The relative weights of C and Si planes depend on the unknown values of $\eta(C)$ and $\eta(Si)$. The uncertainty over weighting factors for distance, and for $\eta(C)/\eta(Si)$ ratios, and the neglect of anisotropy and other complexities, prevent us from using the interference effect to interpret binding energies in a quantitative way. In spite of this, it is possible to reach certain tentative conclusions.

Table III shows that the exciton binding energies are 16, 31, and 32.5 meV. We use only the fact that the two larger binding energies are nearly equal and much larger than the third. A look at Figs. 8(a) and 8(b) shows that it is difficult to establish such a pattern of binding energies for minima near $k_z = 4\pi/c$. On the other hand, because N_2 and N_3 have the same carbon L planes, the pattern is a natural one for minima closer to $3\pi/c$, at or near the position indicated by $6H$?. N_2 and N_3 excitons would certainly then have the larger binding energies if $\eta(C) > \eta(Si)$, as might be expected because C is more electronegative. The small N_3-N_2 binding energy difference of 1.5 meV would then be at-

tributed to the effect of the Si planes. We do not wish to place k_z at $L(3\pi/c)$, for there would then be a degeneracy that would reduce the number of distinct phonon energies observed in the exciton luminescence, contrary to the experimental results. In any case L is not a critical point by symmetry, so there is no reason to favor it, as Fig. 3(b) makes clear.

Our tentative placement of k_z for $6H$ SiC is one in which the binding-energy enhancement is largely due to the C planes at $8c_1/4$. This fact can be related to another common criterion for the binding energies. In the stacking sequence $ABCACB$ the A planes are in a local neighborhood CAC or BAB that has the hexagonal (h) stacking of wurtzite. The other planes have a cubic (k) local environment. All SiC polytype stacking orders can be stated as sequences of h and
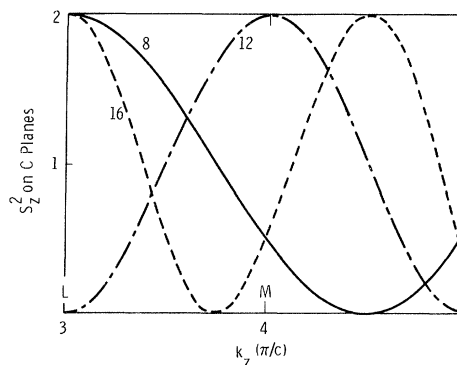

FIG. 7. Plot of $S_z^2 = 2\cos^2 k_z z$ for $z = 8$, 12, or 16 in the units of Table II. Each curve shows the modulation, by S_z^2, of the electron density at a C plane near the donor as a function of the position k_z of the conduction-band minima. No adjustment has been made for distance from the donor.
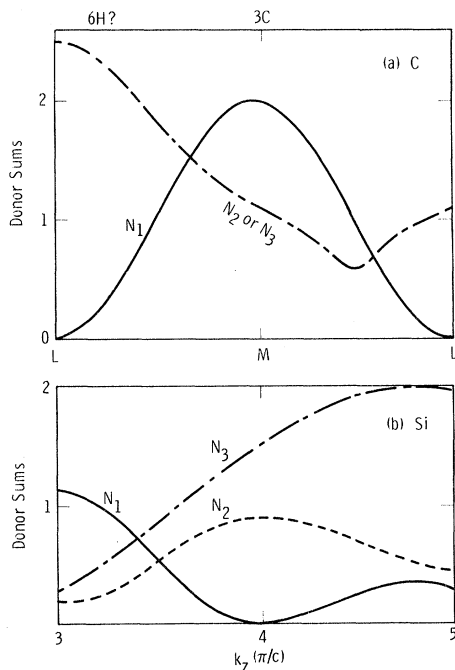
FIG. 8. Weighted sums of S_z^2 for each N donor for (a) carbon L planes, and (b) silicon L planes. The sums are over the planes listed in Table II. These plots are compared with experimental data to suggest a value near $3\pi/c$ for the axial parameter k_z that specifies the positions of the conduction-band minima.

k,[19] and the small binding energies have sometimes been assigned to h sites, the larger energies to k.

Now, any site that has an L plane at $8c_1/4$ is adjacent to an h plane, and is therefore a k site in 6H SiC, which has the stacking sequence hkk. Thus, the two binding criteria give the same answer. However, the rationale for the hk criterion is the difference, as observed along the c axis, between the staggered and eclipsed configurations of two sets of three atoms that lie in planes on either side of the donor plane. This difference could be important for a wave function of C_{3v} symmetry, but not for C_{6v}, which is the symmetry indicated by the Raman-scattering result.

Furthermore, the hk criterion fails for polytype 21R,[28] which has seven inequivalent donor sites, for three small exciton binding energies are observed, although the $hkkhkkk$ stacking order has only two h sites. In this case there are four h neighbors, leaving the observed number of three small binding energies if the $8c_1/4$ planes dominate the binding. However, the importance of $8c_1/4$

planes depends critically on the location of the conduction-band minima, as can be seen in Fig. 7, and there is no information yet on these positions for 21R.

VII. SUMMARY

Raman-scattering results of Colwell and Klein place the conduction-band minima of 6H SiC on the symmetry line M-L, as proposed by Herman *et al.* This is sufficient to determine the planar factor S_p in the Kohn-Luttinger interference effect. For both A_1 and E_2 states, S_p forms patterns of high symmetry in two dimensions. The $A_1(6H)$ pattern is the two-dimensional remnant of the $A_1(3C)$ three-dimensional interference pattern, in which, for a donor on a C site, the electron-density maxima lie on a simple-cubic sublattice of the fcc C sublattice. To fix the positions of the 6H conduction-band minima it is still necessary to find the axial component k_z. The problem is like that of finding k_0/k_{max} for the conduction-band minima of Si.

The ENDOR results for Si fix k_0/k_{max} within close limits. On the other hand, the ENDOR measurements for 6H SiC are insufficient to identify the lattice sites associated with the various resonance lines. The hyperfine splittings have not yet been separated into contact and dipole-dipole parts. Better experimental results would help fix the axial parameter k_z for 6H SiC. In the meantime, a partial evaluation of k_z can be made by studying the binding-energy differences of the three N donors.

The enhancement of the electron binding energy for a donor at one of the three inequivalent sites is due to the concentration of electron density at neighboring lattice sites, first by the portion $u_k(r)$ of the Bloch function, then at sites on L planes by the planar interference factor, and, finally, on the particular L planes favored by the axial interference factor. The differences in binding at the three donor sites are large in 6H SiC because the electron orbit is small, permitting each donor electron to sample a limited and distinct portion of the lattice. The dependence of binding energies on the axial interference factor was used to evaluate k_z by an interpretation of the experimentally observed exciton binding energies. The value of k_z suggested is one for which the number of conduction-band minima is six.

[1]P. J. Colwell and M. V. Klein, in Proceedings of the International Conference on Light Scattering in Solids, Paris, 1971 (unpublished).

[2]E. I. Rashba, Fiz. Tverd. Tela **1**, 407 (1959) [Sov.

Phys. Solid State **1**, 368 (1959)].

[3]F. Herman, J. P. Van Dyke, and R. L. Kortum, Mat. Res. Bull. **4**, S167 (1969). The secondary minima in 2H SiC are also shown by the calculations of H. G. Junginger

and W. van Hearingen, Phys. Status Solidi 37, 709 (1970).

[4]G. Feher, Phys. Rev. 114, 1219 (1959).

[5]E. B. Hale and R. L. Mieher, Phys. Rev. 184, 751 (1969).

[6]T. G. Castner, Jr., Phys. Rev. B2, 4911 (1970), and references therein.

[7]W. Kohn, in Solid State Physics, edited by F. Seitz and D. Turnbull (Academic, New York, 1957), Vol. 5, p. 257.

[8]G. E. G. Hardeman, J. Phys. Chem. Solids 24, 1223 (1963).

[9]D. R. Hamilton, W. J. Choyke, and Lyle Patrick, Phys. Rev. 131, 127 (1963).

[10]A. H. Gomes de Mesquita, Acta Cryst. 23, 610 (1967).

[11]H. H. Woodbury and G. W. Ludwig, Phys. Rev. 124, 1083 (1961).

[12]A. Taylor and R. M. Jones, in Silicon Carbide, edited by J. R. O'Connor and J. Smiltens (Pergamon, New York, 1960), p. 147.

[13]W. J. Choyke, D. R. Hamilton, and Lyle Patrick, Phys. Rev. 133, A1163 (1964).

[14]W. J. Choyke and Lyle Patrick, Phys. Rev. 127, 1868 (1962).

[15]J. L. Birman, Phys. Rev. 115, 1493 (1959); T. K. Bergstresser and M. L. Cohen, ibid. 164, 1069 (1967).

[16]D. W. Feldman, J. H. Parker, Jr., W. J. Choyke, and Lyle Patrick, Phys. Rev. 170, 698 (1968).

[17]H. Jones, in The Theory of Brillouin Zones and Electronic States in Crystals (North-Holland, Amsterdam, 1960), p. 148.

[18]Lyle Patrick, D. R. Hamilton, and W. J. Choyke, Phys. Rev. 143, 526 (1966).

[19]A. R. Verma and P. Krishna, Polymorphism and Polytypism in Crystals (Wiley, New York, 1966).

[20]The electron density on the favored sc sublattice sites is nine time that on the other C sites, omitting any adjustment for distance from the donor.

[21]P. J. Dean and Lyle Patrick, Phys. Rev. B2, 1888 (1970).

[22]This effect would be easier to see in GaP, which also has a zinc-blende lattice with conduction-band minima at X. The $C + S$ pair spectrum is a good one to study as a function of excitation intensity.

[23]There is not a standard notation for representations, and what we call M_3 is sometimes called M_4. We follow the notation of Refs. 2 and 3.

[24]G. B. Wright and A. Mooradian, Phys. Rev. Letters 18, 608 (1967).

[25]There may be three different values of both $\eta(Si)$ and $\eta(C)$ in $6H$ SiC, but this additional complexity will not be considered.

[26]Lyle Patrick and W. J. Choyke, Phys. Rev. B 2, 2255 (1970).

[27]Also, it is not yet certain that the luminescence spectrum of Ref. 9 is correctly attributed to exciton recombination at nitrogen ions.

[28]D. R. Hamilton, Lyle Patrick, and W. J. Choyke, Phys. Rev. 138, A1472 (1965).

Photoluminescence Associated with Multivalley Resonant States of the N Isoelectronic Trap in $In_{1-x}Ga_x P$[†]

D. R. Scifres, H. M. Macksey, N. Holonyak, Jr., R. D. Dupuis, and G. W. Zack

Department of Electrical Engineering, Materials Research Laboratory,
and Coordinated Science Laboratory, University of Illinois at Urbana-Champaign, Urbana, Illinois 61801

and

C. B. Duke, G. G. Kleiman, and A. B. Kunz

Department of Physics, Materials Research Laboratory, and Coordinated Science Laboratory,
University of Illinois at Urbana-Champaign, Urbana, Illinois 61801

(Received 7 October 1971)

Line emission above the direct interband threshold is observed at 77 °K in $In_{1-x}Ga_xP$: N for $0.59 \leq x \leq 0.71$. This emission is identified with a resonance state of the N isoelectronic trap whose properties are evaluated by standard solid-state scattering theory. For $x \geq 0.71$ the nitrogen trap state lies below both the direct and indirect interband thresholds. In this case the sharp, fast, nitrogen A line can be distinguished clearly from the slower, broad N-N pair spectra.

I. INTRODUCTION

In a recent Letter[1] we reported photostimulated line emission above the direct interband threshold associated with a resonance state of the N isoelectronic trap in $GaAs_{1-x}P_x$. It was suggested that a firm confirmation of the interpretation of these earlier data[1] would be the observation of a similar phenomenon in $In_{1-x}Ga_xP$: N for $x \sim 0.7$. In this paper we report such an observation. In addition, the data and theory reported earlier for $GaAs_{1-x}P_x$: N are extended in several directions for the system $In_{1-x}Ga_xP$: N, $0.5 < x \leq 1.0$. First, the photoluminescence spectra are compared with absorption spectra to identify the energy of the band edge in our samples. Because the N state is above